

Predictive Model for Rotating Detonation Engine Wave Structure

Robert F. Burke

The Johns Hopkins University Applied Physics Laboratory
Laurel, Maryland, United States

Taha Rezzag

University of Central Florida
Orlando, Florida, United States

1 Introduction

The Rotating Detonation Engine (RDE) is a novel type of propulsion system that utilizes continuous propagating detonation wave(s) to enable near steady state pressure gain combustion. As opposed to traditional combustors which use deflagration, the RDE has several benefits that include more compact engine size, higher theoretical thermodynamic efficiency, and rapid combustion timescales [1]. The RDE can be geometrically simple when compared to other pressure gain combustion devices [2], but the major research gaps preventing it from advancing in TRL relate to the complex internal flow field from the rotating detonation wave(s) and their ancillary effects inlets, turbines, and nozzles.

The internal flow field of the RDE is unique compared to other detonation devices due to the curvature of the annulus combustion channel and the pressure relief at the exit of the annulus. This complex internal flow field has been shown computationally [3] and experimentally [4]. There are several prominent flow field features that appear in most RDE operation [5,6]. These are the detonation wave front, the refill zone, and the trailing oblique shock and shear layer. These features make up the RDE wave structure that is repeated around the annulus for the number of propagating waves. Previous research shows that the wave structure can change depending on a combination of flow parameters [7] but there are no definitive connections that show the cause of the wave structure variability. Current research considers the detonation wave structure and number of propagating waves as complex and fairly unpredictable characteristics of the RDE and have thus employed data-driven modeling and machine learning [8] to find correlations between the wave structure and some parameters of the engine performance.

This paper proposes a model of the physical sources for the wave structure. This model can predict the geometry of the wave structure and number of detonations based solely on the geometry of the RDE and the inlet flow conditions. Results from this model are compared to published computational and experimental data showing wave structure. Further analysis is made with various propellants and RDE geometry.

2 Methods

The wave structure in the RDE can be broken down into the previously mentioned features: detonation wave, refill zone, oblique shock, and shear layer. These features in the wave structure are shown in Figure 1 for the cylindrical coordinate frame of the RDE. Each feature can be described by an angle relative to the θ axis. These angles are (respectively): α for the detonation wave, β for the refill zone, δ for the oblique shock, and σ for the shear layer.

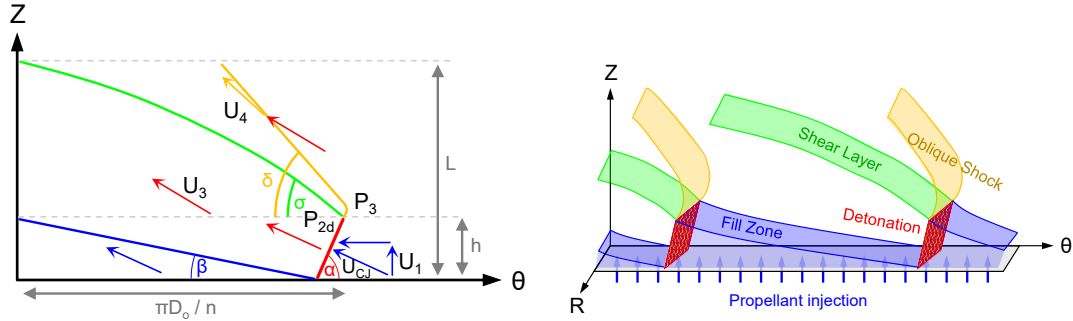


Figure 1: Wave structure diagram (left) and features (right) in the cylindrical coordinate frame.

The detonation wave propagates at the appropriate speed to consume sufficient propellants to continue propagating, like self-sustaining shock wave. In a static laboratory frame, this is seen as the detonation wave propagating through a quiescent mixture at the Chapman-Jouguet speed U_{CJ} . In the static detonation frame, this is seen as the propellant mixture speeding at U_{CJ} into the detonation wave. In the case where the detonation wave is being fed propellants below U_{CJ} , the wave will seek more propellant elsewhere. In the case of the RDE, this is exhibited in its rotational propagation around the annulus. When viewing the detonation wave from the static detonation frame, the oncoming propellant is first moving with some speed U_1 from the injectors and must result in U_{CJ} perpendicular into the wave. For the sake of this analysis, the injectors are solely latitudinal in the z axis. Shown in Figure 1, this essentially slants the detonation wave forward to angle α , such that $\alpha = \cos^{-1}(U_1/U_{CJ})$. Thus, for $U_1 = 0$, or a quiescent mixture, $\alpha = 90^\circ$ and propagates directly in the θ axis like in a linear detonation tube. Alternatively, for $U_1 = U_{CJ}$, or a supersonic/hypersonic propellant injection, $\alpha = 0^\circ$ and exhibits no rotationality, akin to a standing detonation wave engine. In real situations, the detonation wave will look convex with some changing angle α moving away from the injectors which is a result of the decreasing velocity further downstream of the injectors.

Next, the refill zone consists of the region of fresh propellants injected into the RDE for the subsequent detonation wave to consume. This zone can be described by angle β and can be determined from the distance between neighboring detonation waves. In the case of a single detonation wave, this distance is the circumference of the annulus πD_o . In the case of multiple detonation waves, this becomes $\pi D_o/n$, thus being a function of the number of detonation waves n . As such, this paper proposes the Height-Mass-Number (HMN) Correlation. Prior research had developed an equation using channel width and mass flow rate of propellants to estimate the number of detonation waves [9,10]. However, this assumes some critical length that varies with different propellants. The HMN Correlation proposes that this critical length corresponds to a maximum total detonation wave height h_{max} derived from detonation cell width λ using the lower bound from the wave height correlation by Bykovskii [11]. Assuming n number of waves, their individual wave heights h must sum up to h_{max} , represented in Equation 1, where \dot{m}_{total} , ρ , and w (respectively) are total mass flow rate, propellant density, and annulus channel width.

$$nh \leq h_{max} = 11 * 0.7 * \lambda; \text{ for } h = \frac{\dot{m}_{total}}{n\rho w U_{CJ}} \quad (1)$$

The HMN Correlation sensitivity to total mass flow rate can be shown in Figure 2 with an example set of parameters. The number of waves is dependent on the RDE propellants, geometry, and total flow conditions, and thus the refill zone angle β is dependent on the same parameters, such that $\beta = \tan^{-1}((nh)/(\pi D_o))$. The refill zone is critical to the stable propagation of the detonation waves in the RDE. Prior research has shown for stable wave propagation, a balance is required between the detonation velocity and the refill timescale, both a function of the refill zone size and propellant chemistry [12]. Additionally, in real situations, the angle β will be larger as this model does not account for the truncation of the refill zone due to the injector blockage from the high post-detonation pressures. The refill zone does not start immediately after the detonation passes but actually after some distance when the pressure has dissipated and the injectors are unblocked. This results in a shorter refill zone distance between detonation waves and thus a larger β .

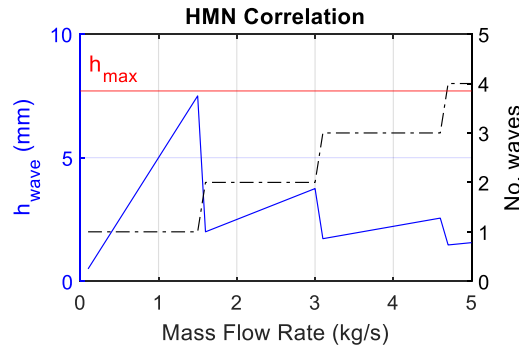


Figure 2: HMN Correlation for example parameters: $U_{CJ} = 2000 \text{ m/s}$, $U_1 = 300 \text{ m/s}$, $\rho_1 = 1 \text{ kg/m}^3$, $w = 100 \text{ mm}$, and $\lambda = 1 \text{ mm}$.

The oblique shock originates from the high-pressure detonation wave, diverting the propellants similarly to a ramp. The oblique shock can be described by angle δ which can be calculated from the pressure ratio across the base of the oblique shock by the detonation wave. This pressure ratio is the immediate post-detonation pressure P_{2d} and the post-combustion products pressure P_3 . In the static detonation frame, the post-combustion products are entering the oblique shock at speed U_3 . Converting to Mach number, this speed and pressure ratio can be used in Equation 2 to determine the shock angle relative to the oncoming flow. To determine the oblique shock angle δ , the shear layer angle σ must also be known. As such, this paper proposes that the shear layer angle σ originates from the streamlines of the post-combustion products, which is the angle of U_3 and acts as the interface between the post-combustion products and the post-oblique shocked products. With σ known, δ can now be calculated.

$$\frac{\frac{P_{2d}}{P_3}(\gamma+1)+(\gamma-1)}{2\gamma M^2} = \sin^2(\delta - \sigma) \quad (2)$$

As the product flow passes through the oblique shock, as with any oblique shock, the flow is turned in towards the shock. In the case of the static detonation frame, this results in flow more latitudinal and in the z axis for useful thrust direction. Given this result, a longer annulus length L can result in more times that the flow can be shocked and further turned towards the z axis; however, this becomes a tradeoff as more times being shocked also results in more non-isentropic losses. Additionally, in the case of very strong pressure ratios P_{2d}/P_3 , the oblique shock can locally detach near the detonation wave, seen as an oblique shock angle δ greater than 90° before trailing to an angle equivalent to the Mach angle for the speed U_3 . This phenomenon can be seen computationally [13] and most often with non-air oxidizers that exhibit high detonation pressure ratios.

3 Results

First, the HMN Correlation was validated with RDE experimental data sweeping total mass flow rates from 0.275 – 0.35 kg/s at a constant equivalence ratio of 1.15 in a comprehensive test campaign [14]. Figure 3 shows the comparison in number of waves between HMN and the experimental data.

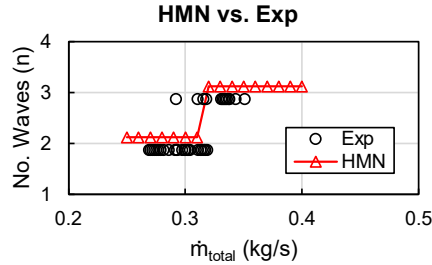


Figure 3: HMN Correlation vs. experimental (Exp) data.

Wave structure parameters were derived from multiple published sources including both computational (*comp.*) and experimental (*exp.*) data of the RDE. Two sources were for a rocket RDE configuration, consisting of the computational work by Lietz et al. [15] and Ross et al. [13]. Another two sources were for air-breathing RDE configurations, consisting of the experimental work by Naples et al. [16] and computational work by Hishida et al. [17]. In each source, wave structure parameters were derived from simulation/experimental images of the detonation wave structure and flow parameters and RDE geometry were given in the references. Table 1 shows these parameters for each source. The H₂-Air detonation cell width λ was assumed to be near 10 mm for stoichiometric flow conditions [18]. Cell width for CH₄-O₂ was sourced from the respective references. Table 2 shows the results comparing the wave structure angles α , β , σ , δ and number of detonation waves n from the HMN Correlation between the sources and the model.

Table 1: Source flow and geometry parameters.

Source	Propellants	Outer Diameter (mm)	Total Mass Flow Rate (g/s)
Lietz et al. (<i>comp.</i>)	CH ₄ -O ₂	76	263
Ross et al. (<i>comp.</i>)	CH ₄ -O ₂	76	270
Naples et al. (<i>exp.</i>)	H ₂ -Air	154	1,380
Hishida et al. (<i>comp.</i>)	H ₂ -Air	200	(0.2 MPa)

Table 2: Wave structure parameters comparison.

Source	α (deg.)		β (deg.)		σ (deg.)		δ (deg.)		n	
Lietz et al.	85.7	82.1	6.9	3.8	20.7	28.1	69.6	68.3	3	2
Ross et al.	85.9	82.1	10.4	3.8	32.2	28.1	68.6	68.4	3	2
Naples et al.	85.6	80.1	13.3	13.7	27.0	32.3	58.0	57.1	1	1
Hishida et al.	79.5	79.9	11.6	7.0	30.3	31.6	56.1	57.0	1	1
	Source	Model	Source	Model	Source	Model	Source	Model	Source	Model

This model could then be used to generate wave structure geometries for any theoretical RDE configurations. The following common propellant combinations were modeled in Figure 4, consisting of H₂-O₂, CH₄-O₂, C₂H₄-Air, H₂-Air. For all propellant combinations, the RDE geometry was the same, $D_o = 150$ mm, $w = 10$ mm, and stoichiometric flow.

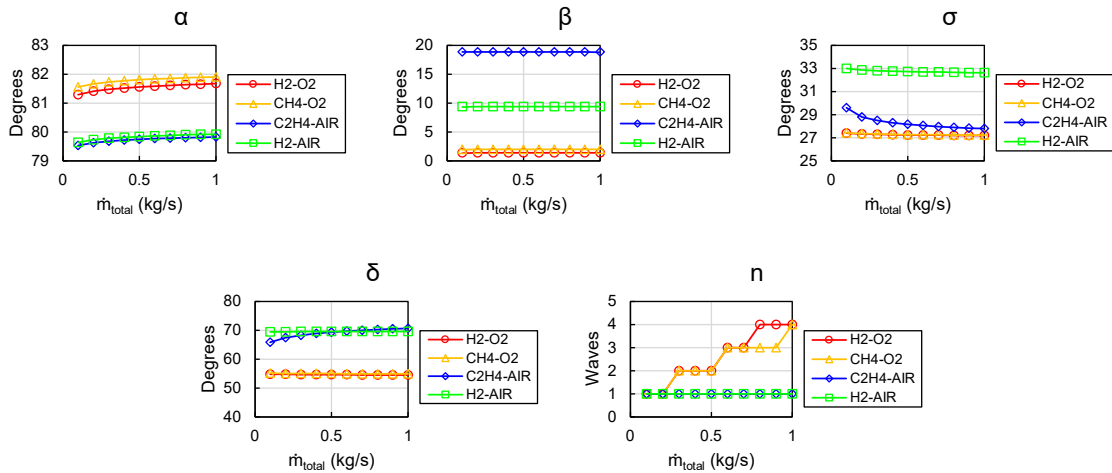


Figure 4: Wave structure parameters for various propellant combinations: H₂-O₂, CH₄-O₂, C₂H₄-Air, H₂-Air.

4 Discussion

Wave structure parameters generated from the model matched decently with both computational and experimental sources for a variety of propellants. Detonation wave angles α were on average within 4% of the source. Refill zone angles β were within 45% and deviated most from their sources when there was a difference in the number of detonation waves n between the source and the model, which is appropriate given β dependence on n . Additionally, β was higher for sources than in the model, supporting the earlier statement in Methods on the effect of injector blockage. Oblique shock angles δ were on average within 2% of the source. Shear layer angles σ were within 35% of the source and were affected by both α and β . The number of detonation waves n was 2 versus 3 for rocket RDE configurations; however, this mass flow rate point was near a transition point according to Figure 3 with experimental data of identical geometry to these sources. The wave numbers matched between the HMN Correlation and the sources for the air-breathing RDE configurations.

Given an accurate representation of the detonation wave structure, performance of the RDE can be generated by stepping through the wave structure and tracking pressure, temperature, and mixture properties according to the newly outlined flow field. The extension of the model in this paper for predicting RDE performance from the wave structure is the topic for future investigations. Such a model could predict RDE performance based only on the RDE geometry, propellants, and flow conditions.

5 Conclusions

This paper proposes a model for predicting the geometry of the detonation wave structure in an RDE based on the RDE geometry, propellants, and flow conditions. Additionally, the physical sources for each feature of the wave structure are explained. As a part of this model, the HMN Correlation was developed which can predict the number of detonation waves from the same RDE parameters. This model was compared to various computational and experimental data with relatively close agreement. The model was used to expand wave structure and wave number to various propellants and RDE geometries. Further work will link engine performance to the wave structure flow field.

Acknowledgments

This material is based upon work supported by internal funding from the Precision Strike Mission Area at Johns Hopkins APL. Author contributions (1) RFB: Idea Generation, Modeling, Paper Writing/Review (2) TR: Idea Generation, Literature Review.

References

- [1] Anand, V., and Gutmark, E., “Rotating Detonation Combustors and Their Similarities to Rocket Instabilities,” *Progress in Energy and Combustion Science*. Volume 73, 182–234. <https://doi.org/10.1016/j.pecs.2019.04.001>
- [2] Wolański, P., “Detonative Propulsion,” *Proceedings of the Combustion Institute*, Vol. 34, No. 1, 2013, pp. 125–158. <https://doi.org/10.1016/j.proci.2012.10.005>
- [3] Raman, V., Prakash, S., and Gamba, M., “Nonidealities in Rotating Detonation Engines,” *Annual Review of Fluid Mechanics*, No. 55, 2023, pp. 639–674. <https://doi.org/10.1146/annurev-fluid-120720>
- [4] Sosa, J., Ahmed, K. A., Fievisohn, R., Hoke, J., Ombrello, T., and Schauer, F., “Supersonic Driven Detonation Dynamics for Rotating Detonation Engines,” *International Journal of Hydrogen Energy*, Vol. 44, No. 14, 2019, pp. 7596–7606. <https://doi.org/10.1016/J.IJHYDENE.2019.02.019>
- [5] Schwer, D., and Kailasanath, K., “Numerical Investigation of the Physics of Rotating-Detonation-Engines,” *Proceedings of the Combustion Institute*, Vol. 33, No. 2, 2011, pp. 2195–2202. <https://doi.org/10.1016/j.proci.2010.07.050>
- [6] Fievisohn, R., and Yu, K. H., “Steady-State Analysis of Rotating Detonation Engine Flowfields with the Method of Characteristics,” *Journal of Propulsion and Power*, Vol. 33, No. 1, 2017. <https://doi.org/10.2514/1.B36103>
- [7] Rankin, B. A., Richardson, D. R., Caswell, A. W., Naples, A. G., Hoke, J. L., and Schauer, F. R., “Chemiluminescence Imaging of an Optically Accessible Non-Premixed Rotating Detonation Engine,” *Combustion and Flame*, Vol. 176, No. January, 2017, pp. 12–22.
- [8] Mendible, A., Koch, J., Lange, H., Brunton, S. L., and Kutz, J. N., “Data-Driven Modeling of Rotating Detonation Waves,” *Physical Review Fluids*, Vol. 6, No. 5, 2021. <https://doi.org/10.1103/PhysRevFluids.6.050507>
- [9] Wolanski, P., “Rotating Detonation Wave Stability,” 2011.
- [10] Connolly-Boutin, S., Joseph, V., Ng, H. D., and Kiyanda, C. B., “Small-Size Rotating Detonation Engine: Scaling and Minimum Mass Flow Rate,” *Shock Waves*, Vol. 31, No. 7, 2021, pp. 665–674. <https://doi.org/10.1007/s00193-021-00991-2>
- [11] Bykovskii, F. A., Zhdan, S. A., and Vedernikov, E. F., “Continuous Spin Detonations,” *Journal of Propulsion and Power*, Vol. 22, No. 6, 2006, pp. 1204–1216. <https://doi.org/10.2514/1.17656>
- [12] Dave, R. T., Burr, J. R., Ross, M. C., Lietz, C. F., and Bennewitz, J. W., “Characteristic Timescales for Detonation-Based Rocket Propulsion Systems,” *Shock Waves*, Vol. 34, No. 2, 2024, pp. 193–214. <https://doi.org/10.1007/s00193-024-01174-5>
- [13] Ross, M. C., Burr, J. R., Desai, Y., Batista, A., and Lietz, C. F., “Flow Acceleration in an RDRE with Gradual Chamber Constriction,” *Shock Waves*, No. 33, 2023, pp. 253–265. <https://doi.org/10.1007/s00193-022-01117-y>
- [14] Bennewitz, J. W., Burr, J. R., Bigler, B. R., Burke, R. F., Lemcherfi, A., Mundt, T., Rezzag, T., Plaehn, E. W., Sosa, J., Walters, I. V., Schumaker, S. A., Ahmed, K. A., Slabaugh, C. D., Knowlen, C., and Hargus, W. A., “Experimental Validation of Rotating Detonation for Rocket Propulsion,” *Scientific Reports*, Vol. 13, No. 1, 2023, pp. 1–13. <https://doi.org/10.1038/s41598-023-40156-y>
- [15] Lietz, C. F., Desai, Y., Munipalli, R., Schumaker, S. A., and Sankaran, V., “Flowfield Analysis of a 3d Simulation of a Rotating Detonation Rocket Engine,” 2019. <https://doi.org/10.2514/6.2019-1009>
- [16] Naples, A., Hoke, J., Karnesky, J., and Schauer, F., “Flowfield Characterization of a Rotating Detonation Engine,” 2013. <https://doi.org/10.2514/6.2013-278>
- [17] Hishida, M., Fujiwara, T., and Wolanski, P., “Fundamentals of Rotating Detonations,” *Shock Waves*, Vol. 19, No. 1, 2009, pp. 1–10. <https://doi.org/10.1007/s00193-008-0178-2>
- [18] Ciccarelli, G., Ginsberg, T., Boccio, J. L., Economos, C., Sato, K., and Kinoshita, M., “Detonation Cell Size Measurements and Predictions in Hydrogen-Air-Steam Mixtures at Elevated Temperatures,” *Combustion and Flame*, Vol. 99, No. 2, 1994, pp. 212–220. [https://doi.org/10.1016/0010-2180\(94\)90124-4](https://doi.org/10.1016/0010-2180(94)90124-4)